AIAA SciTech Forum
6-10 January 2025, Orlando, FL
AIAA SCITECH 2025 Forum

10.2514/6.2025-0809

Instability of Non-Uniformly Curved Deployable Structures

Bowen Li* and Kawai Kwok†
Purdue University, West Lafayette, IN 47907

This paper studies the instability of deployable structures consisting of open-section thin-shells with a non-uniform transverse curvature subjected to pure bending moments. Typically, cylindrical shells have been made from uniformly curved thin-shells for their simplicity, such as tubular extendable booms and tape springs. However, recent consideration has been given to general curved thin-shell structures, which possess a more complex geometry to meet structural and geometric requirements. This paper investigates the buckling instability of two deployable structures: deployable airfoil with continuously varying transverse curvature and deployable boom having a constant-curvature flange and a flat web. An analytical model is presented to predict the buckled cross-section shape based on the variational method. The reaction forces and bending moments are calculated with this analytical model and compared against finite element analysis.

I. Nomenclature

L	=	Strip length for all samples
W_1	=	Chord length of deployable airfoil
W_2	=	Web width of deployable boom
R_3	=	Flange radius of deployable boom
α_3	=	Flange subtending of deployable boom
t	=	Thickness for all samples

II. Introduction

Thin-shell structures are widely used for deployable structures by virtue of their geometrically nonlinear behavior. The classic example is a tape spring, also called carpenter's tape, which is a straight strip with a uniform curved cross-section. The performance of high stiffness during small deflection and compliant behavior after buckling makes this structure attractive for deployable applications. The simplicity of thin-shell structures improves reliability during folding and deployment, eliminates the need for additional support mechanisms, and allows for a compact folded configuration, facilitating easier launching.

The investigation of open thin-shell structures began with analytical developments linking the rotation angle and moment of initially curved strips, which were firstly introduced by Mansfield [1]. These include a transversely and longitudinally curved strip without twist and a twisted strip without initial longitudinal and transverse curvatures, Fig 1(b,c). The transversely curved thin-shell without longitudinal curvature and twisting has received the most widespread attention. It later became known as the tape spring Fig 1(e). A classical shell model with large displacements and large rotations was defined through a dynamic physics-based simulation model, with the equation for the steady-state moment of the tape spring derived theoretically [2, 3]. Based on standard shell theory [4], the buckling behavior and moment-rotation angle relationship under pure bending have been studied theoretically and experimentally [5]. The study later extended the two-dimensional folding of the tape spring to three-dimensional folding. The emphasis was also given to the relationships between moment responses, curvatures, and twist angles [6, 7].

Deployable structures with a non-uniform transverse curvature have been employed for spacecraft masts, including shear-less outrigger booms [8], collapsible tubular mast booms[9, 10] and triangular foldable and collapsible booms [11], shown in Fig 1(f). In these cases, the cross section becomes a symmetrical O and omega shape, or an asymmetrical Y shape. Compared to uniform curved tape spring, these booms have higher bending stiffness performance and multi-stable properties. At the same time, these collapsible and rollable boom can be stowed in a smaller space. However, the

*PhD student, School of Aeronautics and Astronautics.
†Associate Professor, School of Aeronautics and Astronautics, AIAA Associate Fellow, kawaik@purdue.edu

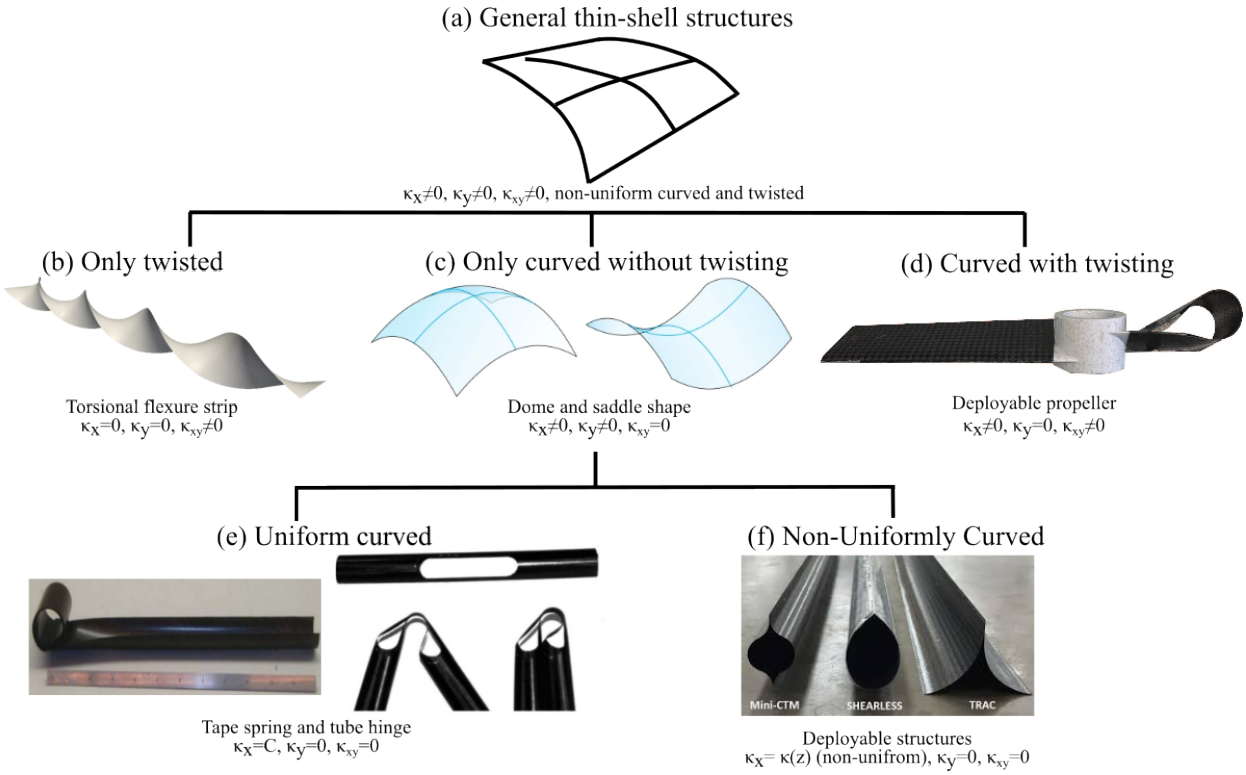

Fig. 1 Different deployable thin-shell structures.

buckling behavior of these structures has not received adequate attention. Buckling can compromise the structural integrity and deployment accuracy, which are crucial for their performance. Specifically, some non-uniform curved thin-shell structures lose their "snap" behavior and convert to limit point buckling due to the non-uniformity of the transverse curvature, which is a critical aspect for ensuring their stability and functionality during deployment.

Deployable structures with a varying curvature are also relevant for aviation applications, such as the recently proposed deployable propeller blade that utilizes buckling to achieve folding [12, 13]. This blade has an airfoil cross-section geometry to generate thrust and lift from the pressure difference during spinning and a spanwise twist.

Present studies are limited to straight and uniformly curved thin-shells. For more general surfaces with non-uniform curvature and twisting, buckling instability is not well understood. These non-uniformly curved thin-shell structures can open up the design space for deployable structures to meet a larger set of geometric and structural requirements. It is important to understand the buckling behavior principle of such complex geometry. This paper aims at developing an analytical model for non-uniformly curved thin-shell structures.

The paper is arranged as follows. Section III shows two deployable structures with non-uniform curvature and explains the analytical model for non-uniform curvature buckling based on variation method. Section IV shows the analytical solution for two samples and the comparison with finite element analysis. Section V concludes the paper.

III. Analysis

Two surfaces were investigated in this paper. The first is a deployable airfoil, which is the top part of NACA 4412 airfoil cross-section, with strip length $L = 200mm$, chord length $W_1 = 50.8mm$, thickness $t_1 = 0.1mm$. The second sample is a deployable boom, which is a half of TRAC boom with strip length $L = 200mm$, flange radius $R_3 = 2mm$, web width $W_2 = 2mm$, thickness $t_2 = t_3 = 0.1mm$, shown in Fig 2. Both of these two samples are non-uniform curved in the transverse direction.

A global coordinate system (X, Y, Z) is specified, where X is normal and vertical to the sample's highest position pointing outward, Y and Z axis correspond to the longitudinal and transverse directions of the sample, respectively. End effects and torsional deformations are neglected under pure bending condition. End effects are neglected, there are no applied surface loads, nor residual stresses. Uniform transverse curvature, denoted by κ_t , is assumed. longitudinal

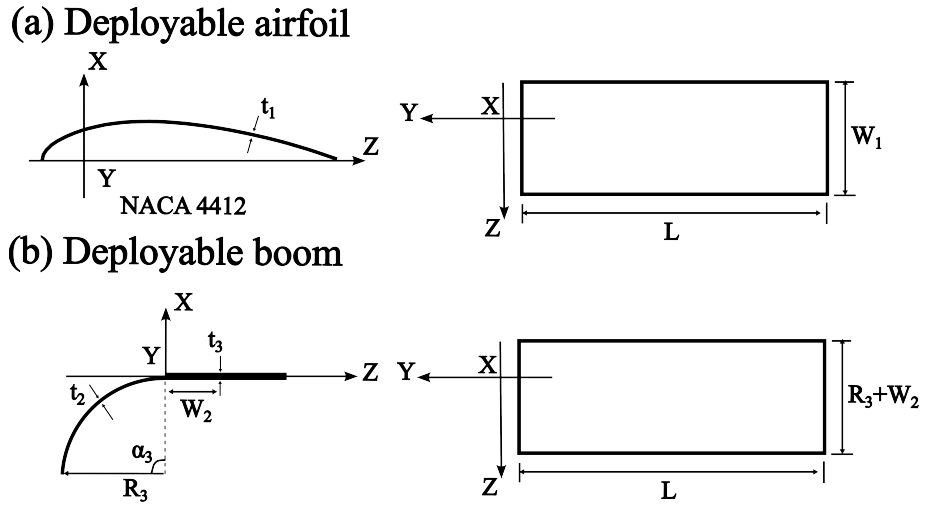

Fig. 2 Geometry model for two strip samples.

curvature is zero. We also neglect torsional deformations.

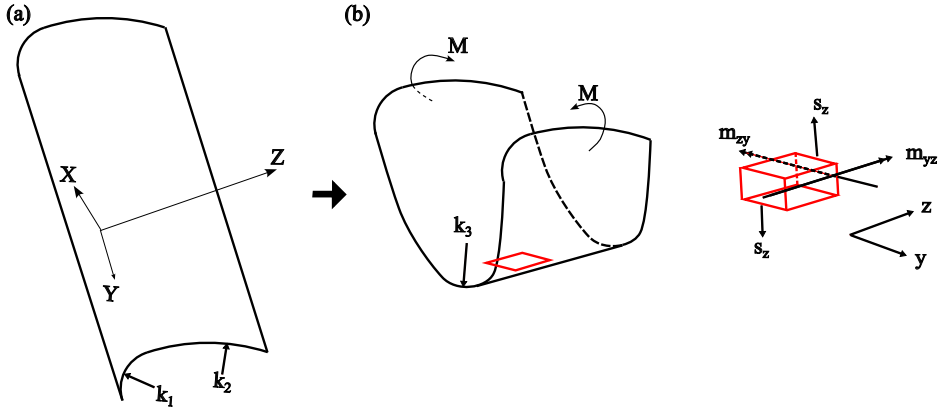

Fig. 3 Definition of coordinate system and stress resultants.

For post-buckling state, we write a general expression for the strain energy density per unit length of the strip. By taking the first variation of strain energy is zero at equilibrium, the governing differential equations for the deformed shape of the cross-section is obtained. This differential equations is then solved subject to boundary conditions under pure bending.

A. Total Strain Energy functional

The strain energy density due to bending is

$$U_b = \frac{D}{2}\left[(\Delta\kappa_t + \Delta\kappa_l)^2 - 2(1-\nu)\Delta\kappa_t\Delta\kappa_l\right] \tag{1}$$

where $D = \frac{Et^3}{12(1-\nu 2)}$, E is Young's modulus and ν is Poisson's ratio. Then, we denote $u(z)$ is the deformed cross-section shape. Then the curvature of the deformed tape spring can be written as a positive second-order derivative of u, $\kappa_{t1} = \left|\frac{d^2u}{dz^2}\right|$. Therefore, the change of transverse curvature is $\Delta\kappa_t = \left|\frac{d^2u}{dz^2}\right| - \kappa_{t0}(z)$. An uniform longitudinal radius, denoted by r_1, is assumed. Because the initial longitudinal curvature is zero, the longitudinal curvature change is $\Delta k_l = \frac{1}{r_1}$. The bending energy density can be expressed as

$$U_b = \frac{D}{2}\left[\left(\frac{d^2u}{dz^2} - \kappa_{t0}(z) + \frac{1}{r_1}\right)^2 - 2(1-\nu)\left(\frac{d^2u}{dz^2} - \kappa_{t0}(z)\right)\left(\frac{1}{r_1}\right)\right]. \tag{2}$$

The strain energy density due to stretching can be calculated by principal in-plane stress resultants, N_t and N_l. There is no stress on the transverse direction, which means $N_t = 0$.

The longitudinal stress is

$$N_l = Et\kappa_l y = \frac{Ety}{r_1}, \tag{3}$$

where y is the vertical distance of a point on the tape spring cross-section from the neutral axis. It is important to notice that $u(z)$ is equivalent to y because we set the coordinate based on neutral axis. The strain energy density is written as

$$U_s = \frac{1}{2Et}\left[(N_t + N_l)^2 - 2(1+\nu)N_tN_l\right] = \frac{N_l^2}{2Et} = \frac{Et}{2r_1^2}u^2 \tag{4}$$

The total energy density is the sum of bending and stretching energy, then integral along the whole cross-section. The total strain energy per unit length of the tape spring is therefore

$$\mathcal{L} = \int_{z_0}^{z_1}\left\{\frac{D}{2}\left[\left(\frac{d^2u}{dz^2} - \kappa_{t0}(z) + \frac{1}{r_1}\right)^2 - 2(1-\nu)\left(\frac{1}{r_1}\right)\left(\frac{d^2u}{dz^2} - \kappa_{t0}(z)\right)\right] + \frac{Et}{2r_1^2}u^2\right\}dz \tag{5}$$

where $\mathcal{L}$ is the total strain energy, z_0, z_1 are the two locations of two edges of the tape-spring.

Consider a small change in total potential energy of the system is given by

$$\delta\Pi = \delta\mathcal{L} - \delta W \tag{6}$$

where W is the external work done. Equilibrium of the system is satisfied when $\delta\Pi = 0$. In the propagation analysis, external work is equated to internal work, thus $\delta\mathcal{L} = \delta W$, hence satisfying $\delta\Pi = 0$. The energy minimization analysis occurs at a fixed extension, setting $\delta W = 0$, and minimizes the internal strain energy by setting $\delta\mathcal{L} = 0$.

B. Variational method

$\mathcal{L}$ is considered as a functional of u, $\frac{d^2u}{dz^2}$, $\kappa_{t0}(z)$. We need to solve $u(z)$ when the functional reaches an extreme value. According to the principle of variational method, the partial differential equation about $u(z)$ is derived by Euler-Lagrange equation.

Calculate all terms based on eq. 5 and substitute into the Euler-Lagrange equation. Simplify the equation with $D = \frac{Et^3}{12(1-\mu^2)}$ and $\gamma^4 = \frac{3(1-\mu^2)}{t^2r_1^2}$. The final partial differential equation for $u(z)$ is:

$$\frac{1}{4\gamma^4}\frac{d^4u}{dz^4} + u = \frac{1}{4\gamma^4}\kappa_{t0}''(z). \tag{7}$$

C. Deformed shape

The homogeneous case is given by

$$\frac{1}{4\gamma^4}\frac{d^4u}{dz^4} + u = 0. \tag{8}$$

A general solution expressing the deformed shape is given by

$$u(z) = C_1\cos\gamma z\cosh\gamma z + C_2\cos\gamma z\sinh\gamma z + C_3\sin\gamma z\cosh\gamma z + C_4\sin\gamma z\sinh\gamma z. \tag{9}$$

Four constants $C_1 - C_4$ need to be determined by four boundary conditions. Form the pure bending boundary condition, the moment m_{zy} and the shear force s_z equal to zero at the two edges of the tape spring. And from standard shell theory, the bending moment per unit length m_{zy} and shear force are related to the changes of transverse and longitudinal curvature by the standard expressions.

$$m_{zy} = D[\frac{d^2u}{dz^2} - \kappa_{t0}(z) + \nu\frac{1}{r_1}] = 0, \quad when \;\; z = z_0 \;\; and \;\; z = z_1 \tag{10}$$

$$s_z = \frac{d^3u}{dz^3} = 0, \quad when \;\; z = z_0 \;\; and \;\; z = z_1 \tag{11}$$

D. End moment

The deformed shape $u(z)$ only depends on the initial strip curvature and the longitudinal curvature after bending. The cross-sectional shape of strip was obtained by solving the differential equation with boundary conditions. The moment per unit length m_{yz} can be calculated by:

$$m_{yz} = D[\frac{1}{r_1} + \nu(\frac{d^2u}{dz^2} - \kappa_{t0}(z))] \tag{12}$$

The end bending moment Mz applied to the strip are obtained by integrating m_{yz} with the effect of normal force over the whole cross-section. Wuest [14] used the following expression:

$$M_z = \int_c (m_{yz} - N_l u(z))\, dz \tag{13}$$

In-plane moment My is the net moment from the normal force N_l along the cross-section about the neutral axis in in Z direction, which is X axis in this coordinate. Therefore, the distance from the normal force N_l to the neutral axis is the z value. We get the net in-plane moment by integral $N_l \cdot z$ about the whole cross-section.

$$M_y = \int_c \frac{Etu(z)}{r_1} \cdot z\, dz \tag{14}$$

IV. Model predictions

A. Airfoil

The initial geometry of NACA 4412 is fitted by polynomial functions at first. Then, the transverse curvature function is obtained by taking the second derivative of these fitted polynomial functions with respect to z. By comparing three to five order polynomial function, the quartic polynomial is chosen for subsequent calculations because it offers higher accuracy and does not overly complicate the subsequent partial differential equations, as shown in Fig. 4.

For a quartic polynomial geometry, the initial curvature is a quadratic function. The right hand side of the partial differential equation equ. 7 is the coefficient of the quadratic term. Consequently, the particular solution is the quartic term coefficient. The solution for the partial differential equation is

$$u(z) = C_1 \cos\gamma z \cosh\gamma z + C_2 \cos\gamma z \sinh\gamma z + C_3 \sin\gamma z \cosh\gamma z + C_4 \sin\gamma z \sinh\gamma z + u_p \tag{15}$$

where u_p is the quadratic term.

B. TRAC boom

The TRAC boom contains two distinct sections with different transverse curvature, $\frac{1}{r_1}$ at the flange section and zero at the web section. Therefore, the transverse curvature about z axis is a piece-wise function.

$$\kappa_{t0}(z) = \begin{cases} \frac{1}{r_1} & z \le 0 \\ 0 & z \ge 0 \end{cases} \tag{16}$$

To simplify the calculation in solving the partial differential equation, the piece-wise function is converted to a non piece-wise function by hyperbolic function. The final transverse curvature function for TRAC boom can be expressed as:

$$k_{t0}(z) \approx \frac{1}{2} * \frac{1 - \tanh(kz)}{R_3} \tag{17}$$

The parameter $k = 10$ is chosen for sharp the steepness of the transition. The right hand side of partial differential equation is zero was assumed.

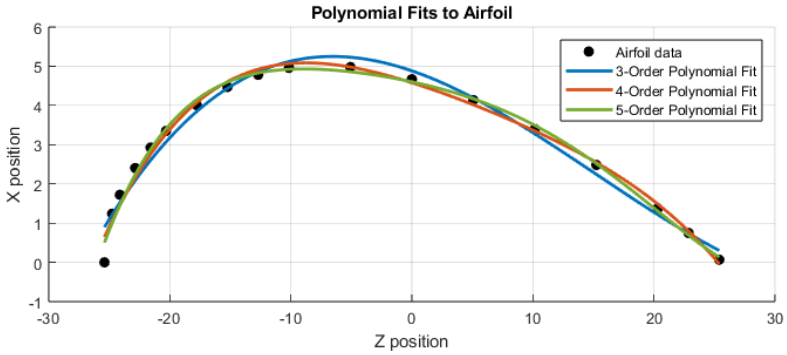

Fig. 4 Airfoil shape polynomial function fitting.

C. Comparison between analytical prediction with finite element model

For a uniformly curved strip, the longitudinal radius after buckling is the same as its original transverse radius. However, this longitudinal radius is an unknown quantity for a buckled non-uniform curved strip. Because different sections with different curvature is trying to buckle to its original curvature to minimize the strain energy. Therefore, the final buckled configuration for non-uniformly curved strip minimizes the net strain energy for the whole structure, which makes the longitudinal radius r_1 after buckling is an unknown quantity in the analytical solution. But this r_1 is a constant during the buckled area propagation. This is similar as a uniformly curved strip, shown in Fig 5.

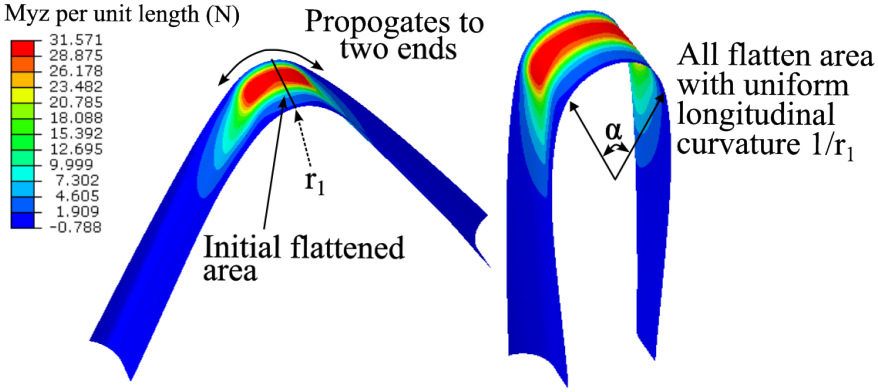

Fig. 5 Buckled area propagates with constant longitudinal curvature.

A group of initial predictions for longitudinal curvature were made based on the original transverse curvature for two samples. All deformed cross-section with different r_1 were obtained. The moment per unit length m_{yz} and m_{zy} were calculated based on equ. 12 and 10. Fig 6 shows the comparison between the analytical predictions with the finite element analysis results.

Table 1 End moments comparison for two samples.

Structures		Analytical prediction (Nmm)	Finite element result (Nmm)	Error
Deployable airfoil	Mz	146.3	146.2	0.1
	Mx	-1.8	-0.2	1.6
Deployable boom	Mz	106.4	106.3	0.1
	Mx	2.3	0.1	2.2

This analytical model predicts that the middle part of two samples are almost flattened. However, this flattened

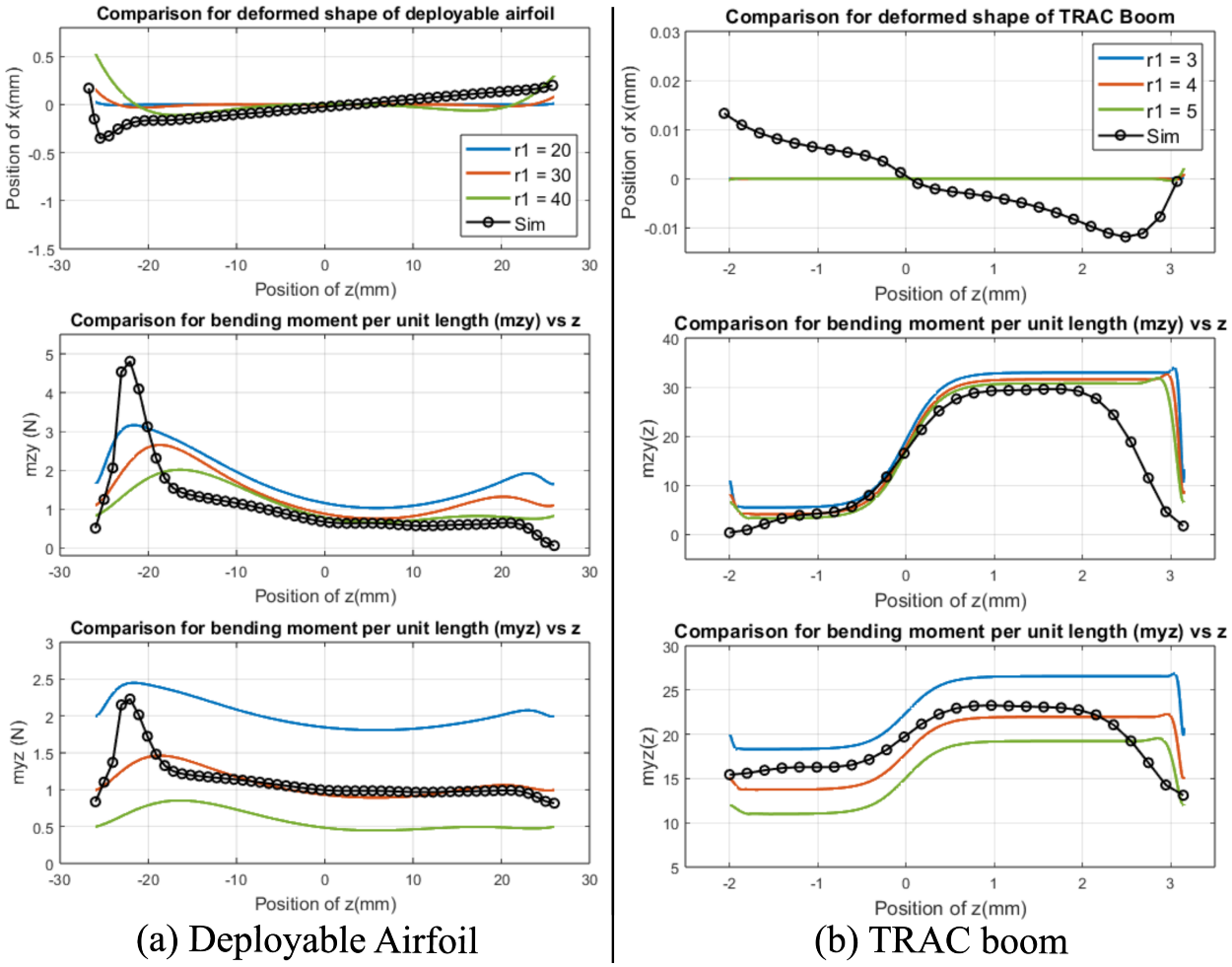

Fig. 6 Comparison for deformed cross-section shape, m_{yz} and m_{zy} for two samples .

cross-section is tilted in simulation for both two samples. This because the longitudinal radius r_1 is not uniform along the transverse direction in simulation. The m_{yz} and m_{zy} followed a similar path with the simulation for both two samples and satisfied the boundary condition $m_{zy} = 0$ at the leading and trailing edges.

By comparing the out-of-plane bending moment M_z and in-plane moment M_x, good agreement was obtained for both the airfoil and TRAC boom, as shown in Table 1. It is important to mention that this in-plane moment M_x is zero for bending a symmetry strip such as tape spring. Because the deformed cross-section and normal force is also symmetry so that the net moment can be canceled.

V. Conclusion

The present paper presents a buckling analysis about non-uniform curved thin-shells under pure bending. Start with the strain energy, an analytical solution for deformed cross-section is given using variation method. It only depends on the second derivative of the original transverse curvature. The normal force, end bending moment and in-plane moment are also derived based on standard shell theory. Two verification samples, a deployable boom and a deployable airfoil, are designed. The buckling behavior non-uniform curvature thin-shell are simulated using the finite element method. Good agreements are observed for the deformed cross-section, end bending moment and in-plane moment.

References

[1] Mansfield, E. H., "Large-deflexion torsion and flexure of initially curved strips," *Proceedings of the Royal Society of London. A. Mathematical and Physical Sciences*, Vol. 334, No. 1598, 1973, pp. 279–298.

[2] Seffen, K., You, Z., and Pellegrino, S., "Folding and deployment of curved tape springs," *International Journal of Mechanical Sciences*, Vol. 42, No. 10, 2000, pp. 2055–2073.

[3] Seffen, K., "On the behavior of folded tape-springs," *J. Appl. Mech.*, Vol. 68, No. 3, 2001, pp. 369–375.

[4] C, C., *Theory of Shell Structures*, Cambridge, London, 1983, Chaps. 14,15.

[5] Seffen, K. A., and Pellegrino, S., "Deployment dynamics of tape springs," *Mathematical, Physical and Engineering Sciences*, Vol. 455, No. 1983, 1999, pp. 1003–1048.

[6] Walker, S. J., and Aglietti, G., "Study of the Dynamics of Three-Dimensional Tape Spring Folds," *AIAA Journal*, Vol. 42, No. 4, 2004, p. 850–856.

[7] Walker, S. J., and Aglietti, G., "A Study into the Dynamics of Three Dimensional Tape Spring Folds," *Journal of Aerospace Engineering*, Vol. 221, No. 3, 2007, pp. 313–325.

[8] Rakow, A. S., Lammers, I., Potter, B., Haynes, A., Tower, S., and Worsdale, C., "Shearless Outrigger Booms with Improved Edge Registration," *AIAA SCITECH 2023 Forum*, 2023, p. 0940.

[9] Fernandez, J. M., Rose, G. K., Younger, C. J., Dean, G. D., Warren, J. E., Stohlman, O. R., and Wilkie, W. K., "NASA's advanced solar sail propulsion system for low-cost deep space exploration and science missions that use high performance rollable composite booms," *International Symposium on Solar Sailing*, 2017.

[10] Lee, A. J., Fernandez, J. M., and Daye, J. G., "Bistable deployable composite booms with parabolic cross-sections," *AIAA SciTech 2022 Forum*, 2022, p. 2264.

[11] Leclerc, C., and Pellegrino, S., "Ultra-thin composite deployable booms," *Proceedings of IASS Annual Symposia*, Vol. 2017, International Association for Shell and Spatial Structures (IASS), 2017, pp. 1–9.

[12] Mashin, A., Li, B., Malyszek, D., Hamillage, M. Y., Kinzel, M., and Kwok, K., "Harnessing instability for deployable propeller blades," *Aerospace Science and Technology*, Vol. 146, 2024, p. 108926.

[13] Li, B., and Kwok, K., "Propagating Instability in Deployable Propeller Blade Structures," *AIAA SCITECH 2024 Forum*, 2024, p. 0272.

[14] Wuest, W., "Einige anwendungen der theorie der zylinderschale," *ZAMM-Journal of Applied Mathematics and Mechanics/Zeitschrift für Angewandte Mathematik und Mechanik*, Vol. 34, No. 12, 1954, pp. 444–454.